AIAA 82-4033

Imperfection Sensitivity of Elastic-Plastic Truss Columns

Esben Byskov*
Technical University of Denmark, Lyngby, Denmark

The sensitivity to local geometric imperfections in the flanges of elastic-plastic truss columns is studied. The analysis utilizes the Shanley tangent modulus concept to determine the load at which the column bifurcates into an overall mode. In order to do so, the reduction in axial stiffness of the flanges due to imperfections and material nonlinearities must be determined. A finite element method is used for this purpose. Previous studies have shown that elastic truss columns exhibit sensitivity to local imperfections, and here it is found that strain hardening plasticity increases this sensitivity. Strain hardening is concluded to be important because application of a Perry first-yield criterion would lead to an underestimation of the carrying capacity.

Nomenclature

A = cross-sectional area of a flange
E = Young's modulus
E_{eff} = effective Young's modulus of geometrically imperfect flange
$\tilde{E}$ = E_{eff}/E
$\tilde{E}^E$ = elastic value of $\tilde{E}$
f_1, f_α = buckling mode amplitudes
$\bar{f}_\alpha$ = imperfection amplitudes
H = distance between flanges
I = moment of inertia of a flange
I_1 = moment of inertia of the truss column
ℓ = bay length of truss
L = length of truss column
n = hardening parameter
N = number of bays
$\bar{P}$ = load unit, see Eq. (3)
r = radius of gyration of a flange
w_1, w_α = buckling modes
$\bar{w}_\alpha$ = imperfections
x = longitudinal coordinate
α = local mode number; range = 2, 3
Δ = shortening of flange member
ϵ = normal strain
ϵ_Y = σ_Y/E
η_α = nondimensional imperfection amplitudes
λ = scalar load parameter
λ_B = value of λ at bifurcation into overall mode for locally imperfect structure
λ_B^E = elastic value of λ_B
λ_P = value of λ at bifurcation for geometrically perfect elastic-plastic structure
λ_Y = σ_Y/σ_E
λ_1 = value of λ at overall buckling of geometrically perfect elastic structure
λ_α = value of λ at local buckling of geometrically perfect elastic structure
λ_1^P = value of λ at overall plastic bifurcation of geometrically perfect structure
λ_α^P = value of λ at local plastic bifurcation of geometrically perfect structure
σ = stress
σ_E = Euler buckling stress of flange member
σ_Y = initial yield stress

Received Jan. 20, 1981; revision received June 29, 1981.

*Associate Professor of Structural Mechanics, Department of Structural Engineering.

Introduction

NONLINEAR interaction between an overall and two local buckling modes causes imperfection sensitivity in elastic truss columns. This result is remarkable because all modes are Euler buckling modes that are imperfection insensitive by themselves. The elastic case has been studied in Refs. 1-3. The present study, which neglects the continuity between the bays of the column flanges, is concerned with the equivalent elastic-plastic problem and can be viewed as an extension of the work of Thompson and Hunt[1] or of Crawford and Hedgepeth.[2] An investigation of a stiffened panel[4] indicates that plasticity increases the imperfection sensitivity. The results for the truss columns agree with this observation.

For elastic structures it usually proves feasible to apply some asymptotic method such as those developed in Refs. 5-7. When the structure experiences plastic strains it is, in general, not possible to establish an asymptotic expansion which covers the geometrically imperfect cases, and it is necessary to resort to numerical methods.

Structural Problem

We consider a simply supported truss column, see Fig. 1, which is long and slender such that the number of bays $N \gg 1$, its length-height ratio $L/H \gg 1$, and such that end disturbances may be ignored. The flanges are, by themselves, assumed to be slender in the sense that $I/(A\ell^2) \ll 1$ where I denotes the moment of inertia of a flange, A its cross-sectional area and $\ell = L/N$ the bay length. Deformation of the column is restricted to its own plane. The column is loaded by an axial load $\lambda\bar{P}$ applied to one of the ends. The load unit $\bar{P}$ will be defined later, and λ is a scalar load parameter. Following Refs. 1-3, we neglect the stiffness of the bracing and adopt the tacit assumption of Refs. 1 and 2 that the flanges have hinges at all nodal points.

In this structure there are three buckling modes that may interact; namely, an overall column buckling mode involving the entire structure and two local column buckling modes confined to the upper and the lower flange, respectively. The overall mode is an Euler mode with wavelength $2L$, and the local modes are Euler modes with wavelength 2ℓ and with the

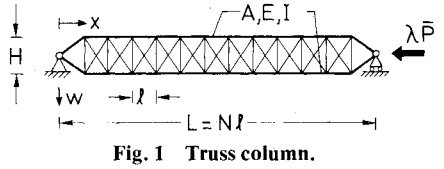

Fig. 1 Truss column.

same amplitude in all bays. We assume that local initial waves in the shape of the local buckling modes comprise the only imperfections, and we take the imperfection amplitude to be the same in both flanges for all bays.

We will consider a loading history during which the load parameter λ is increased slowly from the value 0. During the early stages the column axis remains straight, but at the same time the local buckles grow in size. Whether or not plastic deformation occurs, the resistance to bifurcation into the overall mode is reduced due to the increased waviness of the flanges. When λ reaches a certain value λ_B the column bifurcates into the overall mode. This bifurcation is governed by the "effective" tangent modulus E_{eff} (see Refs. 1 and 2) of the flanges. Application of the Engesser or Shanley column formula then provides the expression

$$\lambda_B \bar{P} = \pi^2 \frac{E_{\text{eff}} I_1}{L^2} \tag{1}$$

with

$$I_1 = 2A(H/2)^2 \tag{2}$$

Elastic Results and Normalizations

It is convenient to take $\bar{P}$ as the load that causes local elastic buckling of the perfect flanges, i.e.,

$$\bar{P} = 2\pi^2 (EI/\ell^2) \tag{3}$$

where E designates Young's modulus. Overall buckling of the geometrically perfect elastic truss is characterized by the value λ_1 of λ

$$\lambda_1 = \frac{1}{4N^2}\left(\frac{H}{r}\right)^2 \tag{4}$$

where

$$r = \sqrt{I/A} \tag{5}$$

is the radius of gyration of a flange. At local elastic buckling the value of λ is

$$\lambda_\alpha = 1, \quad \alpha = 2,3 \tag{6}$$

where $\alpha = 2$ refers to the upper and $\alpha = 3$ to the lower flange, respectively.

From Eqs. (1-5) we get

$$\lambda_B = (E_{\text{eff}}/E)\lambda_1 = \tilde{E}\lambda_1 \tag{7}$$

where

$$\tilde{E} = E_{\text{eff}}/E \tag{8}$$

is a nondimensional effective modulus of elasticity. The value of $\tilde{E}$ is a direct measure of the reduced carrying capacity of the structure. We at this point may emphasize that Eqs. (7) and (8) are also valid in the elastic-plastic case with the remark that λ_1 still designates the elastic overall bifurcation load. It seems reasonable to expect $\lambda_B < \lambda_1$ and also $\lambda_B < 1$.

The transverse components of the modes are

$$w_1(x) = f_1 \sin(\pi x/L) \tag{9}$$

and

$$w_\alpha(x) = f_\alpha \sin(\pi x/\ell) \tag{10}$$

where x is the axial coordinate. As mentioned earlier, we assume that a local initial waviness $\bar{w}_\alpha(x)$ in the shape of the local buckling modes constitutes the only imperfection

$$\bar{w}_\alpha(x) = \bar{f}_\alpha \sin(\pi x/\ell) \tag{11}$$

and that the size of these imperfections is the same in both flanges

$$\bar{f}_3 = -\bar{f}_2 \tag{12}$$

When we introduce the nondimensional imperfection amplitudes $\bar{\eta}_\alpha$ by

$$\bar{\eta}_\alpha = (1/2r)[\bar{f}_2 - (-1)^\alpha \bar{f}_3] \tag{13}$$

where, obviously,

$$\bar{\eta}_3 = 0 \tag{14}$$

we can get the elastic value $\tilde{E}^E$ of $\tilde{E}$ from Ref. 1 or 2 as

$$\tilde{E}^E = [1 + \tfrac{1}{2}(1-\lambda)^{-3}(\bar{\eta}_2)^2]^{-1} \tag{15}$$

Now, the value λ_B^E at elastic bifurcation into the overall mode can be determined from

$$(\lambda_1 - \lambda_B^E)(1-\lambda_B^E)^3 = \tfrac{1}{2}\lambda_B^E(\bar{\eta}_2)^2 \tag{16}$$

Only in the elastic case can we get the analytical expression Eq. (15) for $\tilde{E}$ and, thereby, the analytical expression, Eq. (16), for λ_B.

Elastic-Plastic Case

We take the constitutive relation of the material in the flanges to be elastic-plastic with power law hardening and a continuous tangent modulus

$$\frac{\dot{\epsilon}}{\epsilon_Y} = \frac{\dot{\sigma}}{\sigma_Y} \quad \text{for elastic loading and unloading}$$

$$\frac{\epsilon}{\epsilon_Y} = \left(\frac{1}{n}\left|\frac{\sigma}{\sigma_Y}\right|^n + 1 - \frac{1}{n}\right)\frac{\sigma}{|\sigma|} \quad \text{for plastic loading} \tag{17}$$

Here, σ denotes the stress and ϵ the strain, a subscript Y signifies the value at initial yield, n is the strain hardening parameter, and overdots indicate increments. When $n = 1$, we return to the linearly elastic law, and when $n \to \infty$ we get perfect plasticity.

As in the elastic case we assume moderate displacements and employ a consistent theory with a quadratic measure for the fiber strain. Application of the assumption of plane cross sections and the constitutive law provide the stresses. The normal force and bending moment in the flange member are then found by integration over the cross section. The effective nondimensional tangent modulus $\tilde{E}$ of the imperfect elastic-plastic flange is determined from

$$E = \frac{1}{2}\frac{\bar{P}\ell}{AE}\frac{d\lambda}{d\Delta} \tag{18}$$

where Δ denotes the shortening of the flange member, see Fig. 2. In the numerical computations, we prescribe Δ and for each value of Δ we record the increment $d\lambda$ due to an infinitesimal increment $d\Delta$ of the shortening. In this way we get $\tilde{E}$ as a function of λ for a particular beam with a certain imperfection $\bar{\eta}_2$. We shall later show that the $\tilde{E}-\lambda$ relation provides information about the value of λ_B for a whole range of designs.

In the presence of plastic deformation it is usually necessary to employ some numerical methods such as the finite element method to determine the $\lambda - \tilde{E}$ relation. We base the finite element expressions on the incremental principle of virtual work. In the determination of each $\lambda - \tilde{E}$ curve we use in the order of 50 different values of Δ and iterate at each level until convergence is obtained. Then, for each value of Δ, we perform a computation in which the support at $x = \ell$ is allowed to translate longitudinally. Inversion, or actually factoring, of

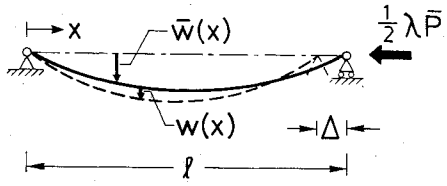

Fig. 2 Geometrically imperfect flange member.

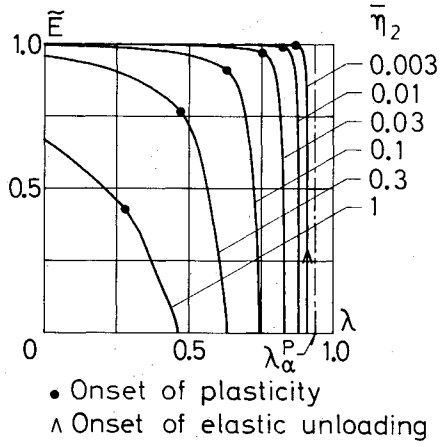

Fig. 3 Effective tangent modulus, $\sigma_Y = 0.9\,\sigma_E$, $n = 3$.

the tangent stiffness matrix for the finite element assembly yields the desired value of $d\lambda/d\Delta$.

The finite elements utilized here employ three degrees of freedom to determine the axial component of the displacement field and four degrees of freedom, namely two rotations and two translations, to determine the transverse component. All nodal displacements will then contribute linearly varying fiber strains in each finite element. We compute the element stiffness and right-hand side matrices by use of Gaussian quadrature. Numerical experience shows that application of four finite elements each with six integration points along the length and eight integration points across the thickness provides ample accuracy.

Numerical Results

In the elastic case the only geometric cross-sectional properties which enter the solution for λ_B are A and I. In the elastic-plastic case the actual shape of the flange cross section constitutes an additional parameter. We have taken the cross section to be square with the side length equal to 1/20 of the bay length ℓ, which leads to realistic structural designs. Another additional parameter is the initial yield stress σ_Y, or rather the ratio λ_Y between σ_Y and the local Euler buckling stress σ_E. It is common practice to make designs such that $\sigma_Y \simeq \sigma_E$ and we have investigated two cases; namely, $\sigma_Y = 0.9\,\sigma_E$ and $\sigma_Y = \sigma_E$. The final additional parameter is the hardening parameter n for which we have taken two values; namely, 3 and 10 characterizing a high and a low hardening material, respectively.

The graph in Fig. 3 covers geometrically imperfect columns which all have $\lambda_Y = 0.9$. Because $\lambda_Y < 1$, their geometrically perfect counterpart has a lowest plastic bifurcation load characterized by a value λ_α^P of λ which lies between λ_Y and 1, discussed later. In spite of the fact that bifurcation at λ_α^P takes place at rising values of λ, we expect that λ for the imperfect columns does not exceed λ_α^P, except for extremely small values of $\bar{\eta}_2$ perhaps. In Fig. 3, λ lies below λ_α^P even for $\bar{\eta}_2$ as small as 0.003. At this point we mention that λ_α^P is also the lowest local plastic bifurcation load for the perfect truss column.

Any point $(\lambda, \bar{E})$ in Fig. 3 can be interpreted as a point at which some reticulated column bifurcates into the overall

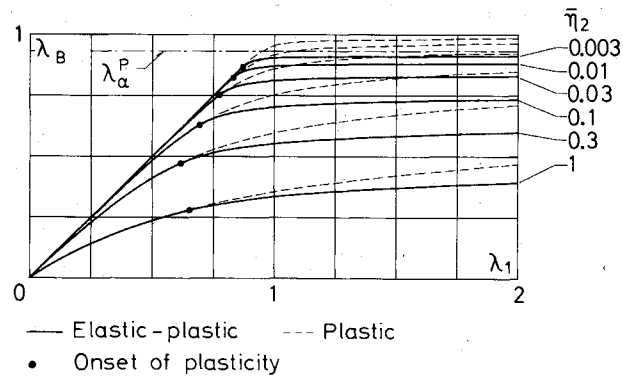

Fig. 4 Carrying capacity of imperfect truss column, $\sigma_Y = 0.9\,\sigma_E$, $n = 3$.

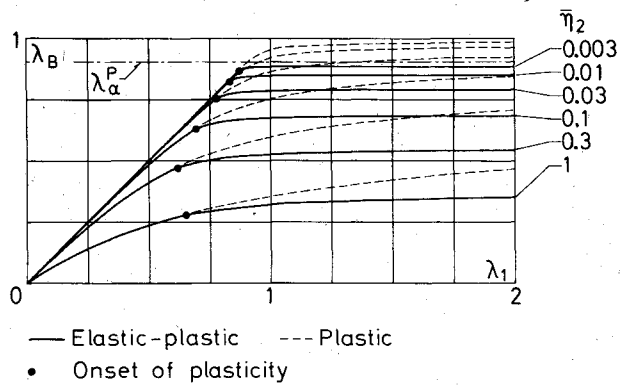

Fig. 5 Carrying capacity of imperfect truss column, $\sigma_Y = 0.9\,\sigma_E$, $n = 10$.

mode. Equation (7) shows that the line $\bar{E} = 1$ corresponds to $\lambda_B = \lambda_I$ and that all points on the line through the origin and $(\lambda_I, 1)$ signify designs with the classical elastic overall buckling load λ_I. Points of intersection between this latter line and the $\bar{E} - \lambda$ curves may, therefore, provide the sought $\lambda_B - \bar{\eta}_2$ relation for a fixed λ_I. When we let the line sweep over the $\bar{E} - \lambda$ diagram, we obtain the plots in Fig. 4.

It is of interest to compare the carrying capacity λ_B of the locally imperfect elastic-plastic truss column with both that of the equivalent elastic structure λ_B^E and with the lowest bifurcation load λ_P of the geometrically perfect elastic-plastic truss column. Equation (16) provides λ_B^E, and λ_P is given by

$$\lambda_P = \min(1,\ \lambda_I,\ \lambda_\alpha^P,\ \lambda_I^P) \tag{19}$$

where λ_I^P denotes the overall plastic bifurcation load. Minor derivations show that

$$\lambda_\alpha^P = \lambda_Y^{(n-1)/n} \tag{20}$$

and

$$\lambda_I^P = \lambda_I^{1/n} \lambda_\alpha^P \tag{21}$$

When $\lambda_Y \geq 1$, λ_P is given by

$$\begin{aligned} \lambda_P &= \lambda_I \quad \text{for} \quad 0 \leq \lambda_I < 1 \\ &= 1 \quad \text{for} \quad 1 \leq \lambda_I < \infty \end{aligned} \tag{22}$$

and otherwise by

$$\begin{aligned} \lambda_P &= \lambda_I \quad \text{for} \quad 0 \leq \lambda_I < \lambda_Y \\ &= \lambda_I^P \quad \text{for} \quad \lambda_Y \leq \lambda_I < 1 \\ &= \lambda_\infty^P \quad \text{for} \quad 1 \leq \lambda_I < \infty \end{aligned} \tag{23}$$

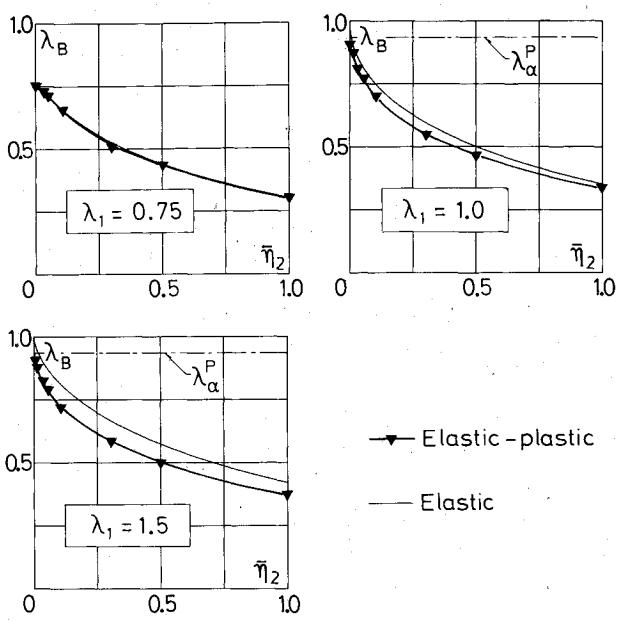

Fig. 6 Sensitivity to local imperfections, $\sigma_Y = 0.9\,\sigma_E$, $n = 3$.

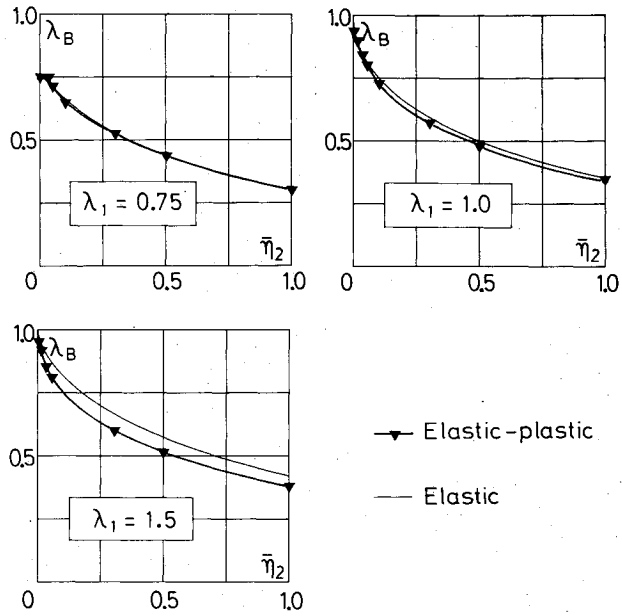

Fig. 8 Sensitivity to local imperfections, $\sigma_Y = \sigma_E$, $n = 3$.

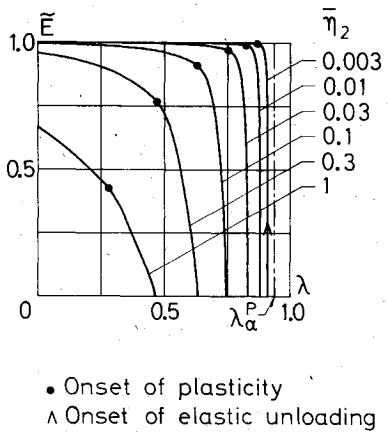

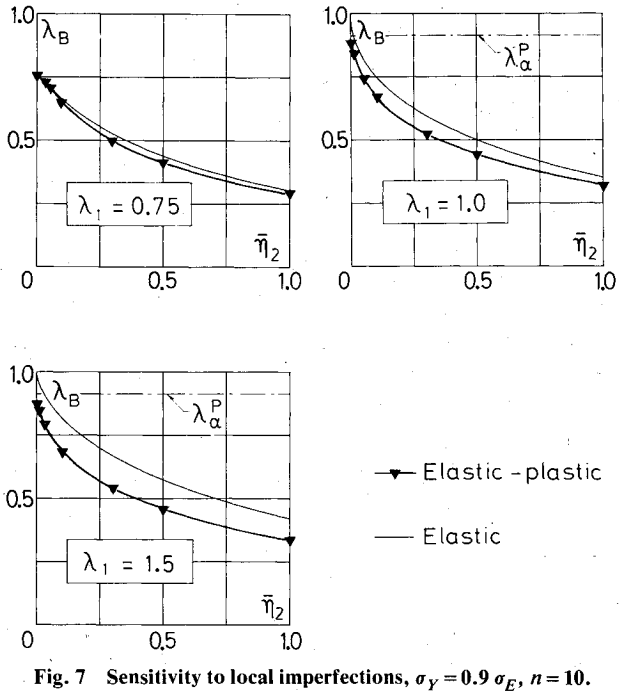

Fig. 7 Sensitivity to local imperfections, $\sigma_Y = 0.9\,\sigma_E$, $n = 10$.

In our examples, the only value of $\lambda_Y < 1$ is $\lambda_Y = 0.9$ yielding

$$\lambda_\alpha^P = 0.9322 \quad \text{for} \quad n = 3$$
$$= 0.9095 \quad \text{for} \quad n = 10 \tag{24}$$

With the value of λ_P in hand, we may divide the reduction in carrying capacity into two parts; namely, the one that is caused by plasticity alone and the remainder that is due to geometric imperfections. In the figures, we have shown λ_α^P but not λ_I^P because λ_I^P only governs in the small interval $0.9 \le \lambda_I < 1$, and we focus attention on three designs outside this range.

It is readily observed from Fig. 4 that plasticity lowers the carrying capacity except for designs with relatively short and stocky flange members, i.e., designs with λ_I less than approximately 0.75. On the other hand, if we adopt a Perry first-yield criterion, see Ref. 8, the plastic branches of the $\lambda_B - \lambda_I$ curves change into horizontal lines emanating from the dots with a considerable overestimation of the imperfection sensitivity as a result. This result holds true even when λ_I is as small as 0.75 provided the imperfection amplitude $\bar{\eta}_2$ is greater than around 0.05-0.1. In the case of a low hardening material characterized by $n = 10$, see Fig. 5, it is, in advance, less obvious that a Perry criterion would provide too pessimistic values for the carrying capacity, but even here the preceding observation holds. From Figs. 6 and 7, plasticity does not change the character of the imperfection sensitivity in that the well known cusp at $\bar{\eta}_2 = 0$ is also present for cases with $\lambda_I \ge$ approximately 1. The similarity between the elastic and the plastic curves is so great that the latter may be obtained from the former simply by subtracting $(1 - \lambda_P)$ for the cases with $\lambda_P < \lambda_I$. This is, however, not the case when $\lambda_Y = 1$ as is seen from Figs. 8 and 9. Here, the cusp on the curves for $\lambda_I \ge 1$ starts at $\lambda_B = 1$, and yet the plastic values lie below the elastic. This implies that the imperfection sensitivity in the plastic case is more severe and more pronounced than when $\lambda_Y = 0.9$.

Both for $\lambda_Y = 0.9$ and for $\lambda_Y = 1$, in all cases with $\lambda_I \ge 1$, the sensitivity to small imperfections, i.e., $\bar{\eta}_2 <$ approximately 0.1, is increased significantly by plasticity. For larger imperfection levels, the absolute value of the reduction relative to the elastic carrying capacity is almost independent of $\bar{\eta}_2$.

Truss columns with other common types of flange cross sections such as circular and I shapes behave somewhat

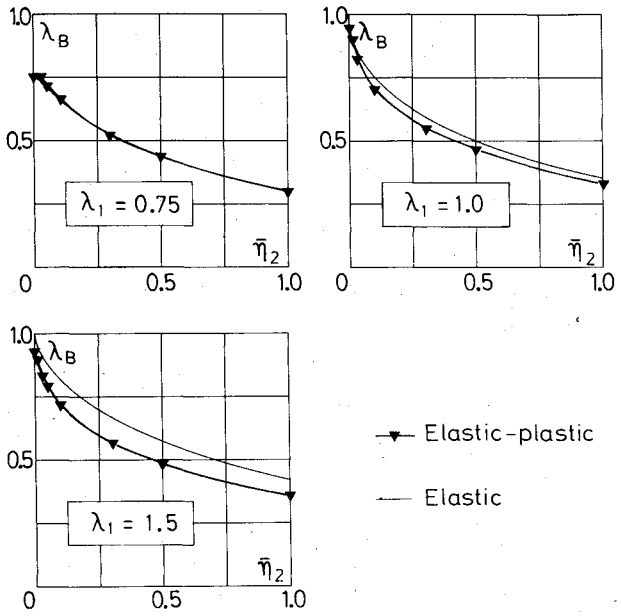

Fig. 9 Sensitivity to local imperfections, $\sigma_Y = \sigma_E$, $n = 10$.

differently from the square used here. For a circular cross section plasticity spreads more slowly and the elastic-plastic results are closer to the elastic values. For an I-shaped cross section, the situation is the opposite because essentially all fibers experience plasticity simultaneously and, consequently, the elastic-plastic curves lie further below the elastic ones than when the cross section is a square. In all cases, however, the behavior is similar to the formerly described.

Overall Imperfections

Overall imperfections which are not treated here can be taken into account by application of Shanley's model to the truss column. The bay in the middle of the column then serves as the elastic-plastic hinge in Shanley's column model. Such a model is consistent with our assumption that the column flanges have hinges at all nodal points.

Conclusions

The foregoing discussion leads to the following conclusions. When plasticity develops it increases the sensitivity to local geometric imperfections. The effect is especially strong for small imperfection levels. Designs with the local Euler buckling stress equal to the initial yield stress suffer a further increased sensitivity. Strain hardening, even when it is low, is important for the carrying capacity because, if it is neglected, then the imperfection sensitivity is overestimated.

References

[1] Thomsen, J.M.T. and Hunt, G. W., *A General Theory of Elastic Stability*, Wiley, New York, 1973, pp. 277-282.

[2] Crawford, R. F. and Hedgepeth, J. M., "Effects of Initial Waviness on the Strength and Design of Built-up Structures," *AIAA Journal*, Vol. 13, May 1975, pp. 672-675.

[3] Byskov, E., "Applicability of an Asymptotic Expansion for Elastic Buckling Problems with Mode Interaction," *AIAA Journal*, Vol. 17, June 1979, pp. 630-633.

[4] Tvergaard, V. and Needleman, A., "Mode Interaction in an Eccentrically Stiffened Elastic-Plastic Panel under Compression," *Buckling of Structures*, IUTAM Symposium, Cambridge/USA, 1974, edited by B. Budiansky, Springer-Verlag, Berlin, 1976, pp. 160-171.

[5] Koiter, W. T. and Kuiken, G.D.C., "The Interaction Between Local Buckling and Overall Buckling on the Behavior of Built-up Columns," Delft Univ. of Technology, Rept. WTHD-23, 1971.

[6] Koiter, W. T., "General Theory of Mode Interaction in Stiffened Plate and Shell Structures," Delft Univ. of Technology, Rept. WTHD-91, 1976.

[7] Byskov, E. and Hutchinson, J. W., "Mode Interaction in Axially Stiffened Cylindrical Shells," *AIAA Journal*, Vol. 15, July 1977, pp. 941-948.

[8] Calladine, C. R., "Inelastic Buckling of Columns: The Effect of Imperfections," *International Journal of Mechanical Sciences*, Vol. 15, July 1973, pp. 593-604.